Diffusion of Interacting Particles in Discrete Geometries

T. Becker,[1,*] K. Nelissen,[2,1] B. Cleuren,[1] B. Partoens,[2] and C. Van den Broeck[1]

[1]*Hasselt University, B-3590 Diepenbeek, Belgium*

[2]*Departement Fysica, Universiteit Antwerpen, Groenenborgerlaan 171, B-2020 Antwerpen, Belgium*

(Received 3 May 2013; published 11 September 2013)

We evaluate the self-diffusion and transport diffusion of interacting particles in a discrete geometry consisting of a linear chain of cavities, with interactions within a cavity described by a free-energy function. Exact analytical expressions are obtained in the absence of correlations, showing that the self-diffusion can exceed the transport diffusion if the free-energy function is concave. The effect of correlations is elucidated by comparison with numerical results. Quantitative agreement is obtained with recent experimental data for diffusion in a nanoporous zeolitic imidazolate framework material, ZIF-8.

DOI: 10.1103/PhysRevLett.111.110601 PACS numbers: 05.40.Jc, 02.50.−r, 05.60.Cd, 66.30.Pa

The equality of inertial and gravitational mass played a crucial role in Einstein's discovery of general relativity. Similarly, Einstein's work on Brownian motion is based on the identity of the transport- and self-diffusion coefficients for noninteracting particles [1], leading eventually through Perrin's experiments [2] to the vindication of the atomic hypothesis. In general, however, diffusion of interacting particles is described by two different coefficients. The transport-diffusion coefficient D_t quantifies the particle flux j appearing in response to a concentration gradient dc/dx:

$$j = -D_t \frac{dc}{dx}. \tag{1}$$

The self-diffusion coefficient D_s describes the mean squared displacement of a single particle in a suspension of identical particles at equilibrium: $\langle x^2(t)\rangle \propto D_s t$. An alternative way for measuring this coefficient is by labeling, in this system at equilibrium, a subset of these particles (denoted by *) in a way to create a concentration gradient dc^*/dx of labeled particles under overall equilibrium conditions. The resulting flux j^* of these particles reads:

$$j^* = -D_s \frac{dc^*}{dx}. \tag{2}$$

Both forms of diffusion have been studied in a wide variety of physical contexts, including continuum [3–10] and lattice [11–13] models. Exact analytical results for the diffusion coefficient of interacting particles are, however, typically limited to a perturbation expansion, for example, in the density of the particles. The effect of correlations is notoriously difficult to evaluate in continuum models, especially when hydrodynamic interactions come into play, while they can play a dominant role, for example, in lattice models with particle exclusion constraints.

In this Letter, we introduce a physically relevant model, for which exact analytical results can be obtained at all values of the concentration and for any interaction. It describes the diffusive hopping of interacting particles in a compartmentalized system, see Fig. 1 for a schematic representation. It is assumed that the relaxation inside each cavity is fast enough to establish a local equilibrium, described by a free-energy function characterizing the confinement and interaction of the particles. This model describes diffusion in confined geometries [14]. Of particular interest are microporous materials [15,16], which are widely used in industry, e.g., as catalysts in petrochemical industry and as water softeners. Because of their high thermal and chemical stability [17] and potential applications including carbon dioxide capture and storage [18] and gas separation [19], zeolitic imidazolate frameworks (ZIFs) have received considerable interest. As illustration, we compare our predictions with experimental results [20] of diffusion of methanol in ZIF-8. At variance with previous experiments [21–26], it was found that the self-diffusion could exceed the transport diffusion, a result confirmed by molecular dynamics (MD) simulations [27–29]. We corroborate the observation that this phenomenon is due to clustering of the particles, and provide an analytical argument and a simple interpretation for the inversion. Our model in fact allows us to reproduce, in a quantitative way, the loading dependence of the self-diffusion and

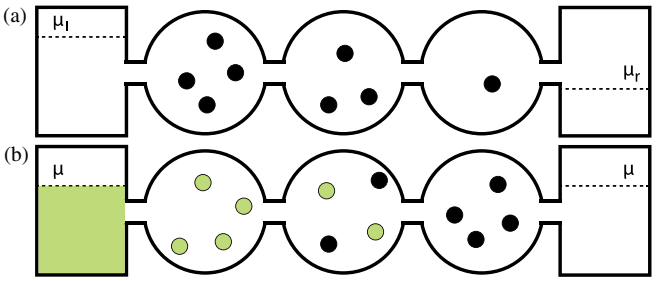

FIG. 1 (color online). The model: particles enter cavities via particle reservoirs at certain chemical potential. Particles jump between different cavities through narrow passages. (a) Transport diffusion: a concentration gradient shows a current. (b) Self-diffusion: a concentration gradient of labeled particles is introduced under overall equilibrium conditions.

transport diffusion for different interactions. Finally, we mention that our model also serves an educational purpose, as the distinction between the transport- and self-diffusion coefficients, and the role and contribution of the correlations therein can be identified explicitly.

The model consists of a one-dimensional array of pairwise connected cavities, with particles entering in the outer left and right cavities from reservoirs at chemical potentials μ_l and μ_r, respectively (see Fig. 1). The entire system is at temperature T. Particles stochastically jump between cavities by moving through narrow passages. These transitions occur on a slow time scale compared to the relaxation time inside each cavity, ensuring that an equilibrium distribution is effectively maintained in each cavity. It is described by a free energy $F(n) = U(n) - TS(n)$, with n the number of particles in the cavity, $U(n)$ the energy, and $S(n)$ the entropy. Furthermore, the dynamics is Markovian with a transition rate which has to reproduce the thermal equilibrium state p^{eq}, when a cavity is connected to a single reservoir at chemical potential μ:

$$p_n^{\mathrm{eq}}(\mu) = (\mathrm{Z})^{-1}\mathrm{e}^{-\beta[\mathrm{F(n)}-\mu\mathrm{n}]}, \tag{3}$$

with $\beta = (k_B T)^{-1}$ and Z^{-1} the normalization constant.

We first derive an exact expression for D_t and D_s, in a limiting situation where correlations between particle numbers in different cavities are absent (see also Supplemental Material [30]). Consider a system consisting of three cavities, with n_l, n, and n_r specifying the number of particles inside the left, middle, and right cavity, respectively. In the limit in which the exchange rates with the middle cavity are small compared to the exchange rates with the reservoirs, the left and right cavity are effectively decorrelated from the middle cavity, and are characterized by the equilibrium probability distribution $p_{n_l}^{\mathrm{eq}}(\mu_l)$ and $p_{n_r}^{\mathrm{eq}}(\mu_r)$, respectively. This setup allows us to obtain exact analytical results at arbitrary particle density. The probability distribution p_n for the middle cavity obeys the following master equation:

$$\dot{p}_n = k_{n-1}^{+} p_{n-1} + k_{n+1}^{-} p_{n+1} - (k_n^{+} + k_n^{-}) p_n, \tag{4}$$

with k_n^{+} and k_n^{-} the rates to add or remove a particle from the middle cavity containing n particles:

$$k_n^{+} = \sum_{n_l} p_{n_l}^{\mathrm{eq}}(\mu_l) k_{n_l n} + \sum_{n_r} p_{n_r}^{\mathrm{eq}}(\mu_r) k_{n_r n}, \tag{5}$$

$$k_n^{-} = \sum_{n_l} p_{n_l}^{\mathrm{eq}}(\mu_l) k_{n n_l} + \sum_{n_r} p_{n_r}^{\mathrm{eq}}(\mu_r) k_{n n_r}. \tag{6}$$

The rate k_{nm} denotes the probability per unit time for a particle to jump from a cavity containing n particles to a neighboring cavity containing m particles. At this stage, we do not need to specify its explicit form, but we request that it obeys detailed balance:

$$k_{nm}/k_{m+1,n-1} = e^{-\beta[F(m+1)+F(n-1)-F(n)-F(m)]}. \tag{7}$$

The particle flux and concentration difference between the left and middle cavity read:

$$j(\mu_l, \mu_r) = \sum_{n,n_l} (k_{n_l n} - k_{n n_l}) p_{n_l}^{\mathrm{eq}}(\mu_l) p_n, \tag{8}$$

$$dc(\mu_l, \mu_r) = (1/\lambda) \sum_{n,n_l} (n - n_l) p_{n_l}^{\mathrm{eq}}(\mu_l) p_n, \tag{9}$$

where λ is the center-to-center distance between cavities. The transport diffusion D_t, quantifying the linear response of j with respect to dc, is found from the ratio $-j/(dc/\lambda)$ in the limit $\delta = (\mu_l - \mu_r)/2 \to 0$. Introducing the average chemical potential $\mu = (\mu_l + \mu_r)/2$, one finds for Eqs. (5) and (6) up to linear order in δ:

$$k_n^{+} = 2\sum_m p_m^{\mathrm{eq}}(\mu) k_{mn}, \qquad k_n^{-} = 2\sum_m p_m^{\mathrm{eq}}(\mu) k_{nm}. \tag{10}$$

One concludes from Eq. (4) that at this order in δ, the steady state solution of the master equation is given by $p_n = p_n^{\mathrm{eq}}(\mu)$. The corresponding current and concentration difference are obtained from the expansion of Eqs. (8) and (9) to first order in δ, resulting in

$$D_t(\mu) = \frac{\lambda^2 \sum_{n,m} p_n^{\mathrm{eq}}(\mu) p_m^{\mathrm{eq}}(\mu) k_{nm}}{\langle n^2 \rangle - \langle n \rangle^2} \equiv \frac{\lambda^2 \langle k \rangle}{\langle n^2 \rangle - \langle n \rangle^2}, \tag{11}$$

where $\langle \cdot \rangle$ denotes the average over $p^{\mathrm{eq}}(\mu)$.

We next turn to the self-diffusion, using the labeling procedure discussed in the introduction. Since the final expression for D_s does not depend on the labeling percentages, we consider a simple case: all particles in the left reservoir are labeled, those in the right reservoir remain unlabeled. As a result, all particles in the left and none in the right cavity are labeled. The state of the middle cavity is now described by two numbers, n (total number of particles) and n^*, the number of labeled particles. The corresponding steady state probability distribution p_{n,n^*} is

$$p_{n,n^*} = p_n^{\mathrm{eq}}(\mu) \frac{n!}{n^*!(n-n^*)!} \frac{1}{2^n}. \tag{12}$$

The flux of labeled particles and concentration difference between the left and middle reservoir read

$$j^* = \sum_{n_l,n,n^*} \left(k_{n_l n} - k_{n n_l} \frac{n^*}{n} \right) p_{n,n^*} p_{n_l}^{\mathrm{eq}}(\mu) = \frac{\langle k \rangle}{2},$$

$$dc^* = (1/\lambda) \sum_{n_l,n,n^*} (n^* - n_l) p_{n,n^*} p_{n_l}^{\mathrm{eq}}(\mu) = -\langle n \rangle/2. \tag{13}$$

Hence, the self-diffusion $D_s = -j^*/(dc^*/\lambda)$ reads

$$D_s(\mu) = \lambda^2 \langle k \rangle / \langle n \rangle. \tag{14}$$

Equations (11) and (14) constitute the main analytical results in this Letter. They are valid at all values of the concentration and can be calculated for any interaction. From Eqs. (11) and (14), one finds for the ratio of D_t and D_s:

$$\frac{D_t(\mu)}{D_s(\mu)} = \frac{\langle n\rangle}{\langle n^2\rangle - \langle n\rangle^2} = \frac{\langle n\rangle}{\mathrm{Var}(n)} = \Gamma(\mu), \qquad (15)$$

where $\Gamma(\mu)$, the so-called thermodynamic factor, is an equilibrium property. Equation (15) can be derived by a general argument, when correlations are ignored [11,12]. We note that Eqs. (11) and (14) remain valid for any number of cavities between the left and right cavities, provided correlations in particle number are ignored [31].

We now comment on the effect of interaction, and in particular of the shape of the free energy, on the thermodynamic factor. In the absence of interactions, the free energy is that of an ideal gas $\beta F^{\mathrm{id}}(n) = \ln(n!) + cn$, with c a constant [32]. The corresponding distribution $p_n^{\mathrm{eq}}(\mu)$ is Poissonian for which $\langle n\rangle = \mathrm{Var}(n)$ and hence $\Gamma = 1$. One recovers the "Einstein" result that $D_s = D_t$ for noninteracting particles. Note that adding an arbitrary linear term $\propto n$ to $F(n)$ corresponds to a rescaling of the chemical potential, see Eq. (3). Hence, a linear term in $F(n)$ does not influence the statistics at a given loading $\langle n\rangle$. We now show that for deviations of the free energy from the ideal gas value, $f(n) = F(n) - F^{\mathrm{id}}(n)$, the ratio of D_t and D_s is determined by the convexity versus concavity of $f(n)$, where we will call $f(n)$ the interaction free energy. We fix the loading $\langle n\rangle$ and consider two neighboring cavities containing, respectively, n_1 and n_2 $(> n_1)$ particles. A particle now jumps so that the new state becomes $n_1 - 1$ and $n_2 + 1$. Such an event increases the local density inhomogeneity. When $f(n)$ is convex $[f''(n) > 0]$, the interaction free energy is larger in the new state: $f(n_1) + f(n_2) < f(n_1 - 1) + f(n_2 + 1)$. Therefore, its probability is small compared to the situation with no interactions. $\mathrm{Var}(n)$ decreases since particle numbers different from the average loading become less probable. Hence, when $f(n)$ is convex, $\mathrm{Var}(n) < \langle n\rangle$, $\Gamma > 1$, and $D_t > D_s$. When $f(n)$ is concave $[f''(n) < 0]$ the opposite happens. The interaction free energy of the new state is smaller and both its probability and $\mathrm{Var}(n)$ increase, leading to $\Gamma < 1$ and $D_t < D_s$.

A few additional remarks are in order. First, a cavity can typically contain a limited number of particles $n \le n_{\max}$. This corresponds to $f(n) = \infty$ for all $n > n_{\max}$, i.e., $f(n)$ is "infinitely convex" at $n_{\max}$. We conclude from the above argument that a concave section is a necessary, but not sufficient, condition for having $\mathrm{Var}(n) > \langle n\rangle$, i.e., for D_s to exceed D_t. Second, one can give an intuitive explanation as to why a concave $f(n)$ promotes $D_s > D_t$. D_t is measured by a flux j. If $f(n)$ is concave, particles tend to cluster, which will mostly happen in cavities that are already high in particle number. This causes the particles to be "pulled back" towards the region of higher concentration. The net effect is a force in the direction of higher concentration, lowering the particle flux. D_s is measured by a flux of labeled particles j^*. Since the system is in equilibrium there is no concentration gradient. As a result, there is no preferential direction for clustering, and there will be no force counteracting the current of labeled particles. Finally, the experimental finding of D_s exceeding D_t [20] was explained on the basis of MD simulations [27–29] as due to clustering of particles. Our model corroborates this conclusion but, in addition, provides a simple physical interpretation and an analytical argument.

For systems containing an arbitrary number of cavities, one has to take into account correlation effects. Finding an exact solution becomes difficult. Instead, we have performed kinetic Monte Carlo simulations (see Supplemental Material [30]). Our choice of rates is

$$k_{nm} = \nu n e^{-(\beta/2)[f(n-1)+f(m+1)-f(n)-f(m)]}. \qquad (16)$$

The factor ν determines the time scale. In the limit of infinite dilution, both D_t and D_s are equal to $\nu\lambda^2 \equiv D_0$. For an ideal gas $f(n) = 0$, $k_{nm} = \nu n$, i.e., the rates satisfy the law of mass action [33]. The simulations presented here are for 15 pairwise connected cavities, with $n_{\max} = 13$. D_s/D_0, D_t/D_0, and Γ^{-1} are plotted in Fig. 2 for different types of free energies, as a function of the loading $\theta = \langle n\rangle/n_{\max}$. Both the simulation data and the analytical curves of Eqs. (11) and (14) are shown. The stars in the figures correspond to the ratio between the self- and transport diffusion obtained from simulations. Since correlations are included in the simulations but are absent in the analytical result, the difference of the two curves is a measure of the effect of correlations on the diffusion. Figure 2(a) shows the diffusion for noninteracting particles $\beta f(n) = 0$, with confinement (presence of $n_{\max}$). At low and medium loadings the particles are not influenced by the

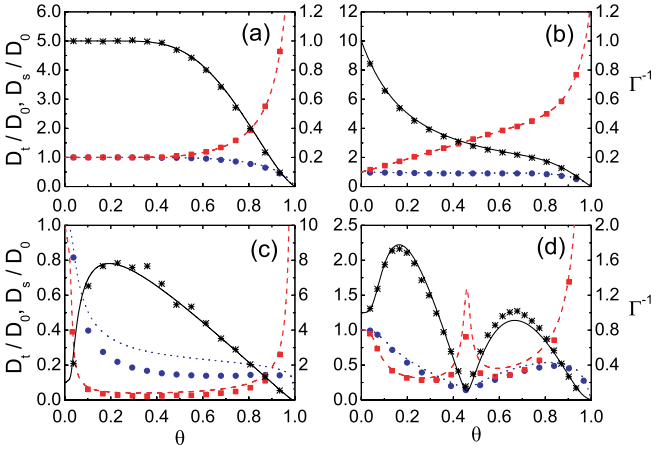

FIG. 2 (color online). D_s/D_0, D_t/D_0, and Γ^{-1} as a function of loading $\theta = \langle n\rangle/n_{\max}$, $n_{\max} = 13$; for (a) $\beta f(n) = 0$, (b) $\beta f(n) = 0.2n^2$, (c) $\beta f(n) = -0.2n^2$, and (d) $\beta f(n)$ that is subsequently concave, convex, and again concave. The red dashed lines (analytical solution) and squares (simulations) show the transport diffusion, and the blue dotted lines (analytical solution) and full circles (simulations) the self-diffusion (values on lhs axis). The analytical Γ^{-1} (black full lines) are compared with the ratio of D_s and D_t (black stars) from the simulations (values on rhs axis).

confinement; $\Gamma = 1$ and $D_s = D_t$. At high loading, the confinement comes into play: Γ^{-1} decreases, D_t rises, and D_s lowers. The effect of correlations is negligible: the simulation data and analytical results coincide almost perfectly. Figure 2(b) shows the diffusion in the case of a convex free energy $\beta f(n) = 0.2n^2$. Γ^{-1} is lower than one, and D_t is always larger than D_s. Correlations have a negligible influence. Figure 2(c) shows the diffusion for a concave free energy $\beta f(n) = -0.2n^2$. As expected, $D_s > D_t$ for low to moderate loading. At moderate and high loading the "convexity effect" of confinement takes over: Γ^{-1} decreases and eventually becomes smaller than one with $D_t > D_s$. This curve should be compared with Figs. 3(a) and 3(c) in [20]. Noteworthy is the fact that the transport diffusion shows a minimum when the thermodynamic factor is around its maximum. This feature is in agreement with experimental observations [20,34,35] and with MD simulations [36]. It is now easily understood: when Γ^{-1} is at its highest, the tendency to cluster is maximal, therefore, the force opposing the current is also at its strongest. Turning to the effect of correlations, we note that they are quite strong: both D_t and D_s are significantly lower than the analytical results. The effect is the largest for self-diffusion. Nevertheless, the ratio of D_t and D_s is still very close to Γ, again in agreement with what is observed in experiments [20] and MD simulations in similar systems [37]. Figure 2(d) shows the diffusion for a free energy that is first concave, then convex and then concave (see Supplemental Material [30] for the exact form). For the first concave part, the self-diffusion exceeds the transport diffusion. For the second concave part, this is no longer the case, due to the confinement and the influence of the convex part in the middle. This is an illustration of how concavity is necessary but not sufficient for $D_s > D_t$. D_t shows a (local) maximum in the convex part, whereas D_s shows a (local) minimum. Correlations have noticeable effect, and are now more important for D_t than for D_s. Notice that in all cases correlations lower the diffusion coefficients.

Motivated by the qualitative agreement with experiments, we have tried to reproduce the experimental results from [20] quantitatively. Inspired by the form of the energy function for Lennard-Jones crystals [38], we take $\beta f(n) = an^2 + bn^3$ for $n \leq n_{\max}$, with $n_{\max} = 13$ taken from the experimental data [39]. The parameters a and b are determined by fitting the thermodynamic factor [Eq. (15)] with the experimental data, resulting in $\beta f(n) = 0.000\,642n^2 - 0.0083n^3$. The parameters ν and λ only appear in the combination $\nu\lambda^2$, which follows directly from the experimental value of D_t at very low loading. In Fig. 3, we compare the obtained simulation results for D_s and D_t with experimental data of methanol in ZIF-8 [39]. Quantitative agreement is found for both D_s and D_t at all values of the loading. This is remarkable since a and b are determined from the equilibrium quantity Γ, and only the

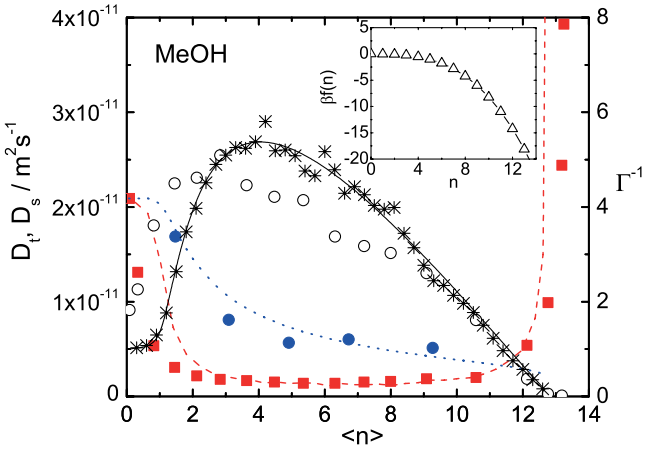

FIG. 3 (color online). Comparison of experimental data of methanol in ZIF-8 [39] with simulations from our model. The experimental self-diffusion and transport diffusion are represented by the blue full circles and red squares, respectively, with the corresponding results from simulations given by the blue dotted line and the red dashed line (values on lhs axis). The experimental (black open circles) and analytical (full black line) Γ^{-1} are compared with the ratio of self- and transport diffusion (black stars) taken from the simulations (values on rhs axis). The inset shows $\beta f(n)$.

experimental value of D_t at very low loading is used in the fit of $\nu\lambda^2$. A similar quantitative agreement is also found for ethanol in ZIF-8 (cf. Supplemental Material [30]).

To conclude, we have introduced a model describing diffusion of interacting particles in discrete geometries. Exact analytical expressions for the self- and transport diffusion are given in the limiting case where correlations are absent, but are otherwise valid at all values of the concentration and for any interaction. We showed that the self-diffusion can exceed the transport diffusion when the free-energy function is concave as a function of the loading, resulting in the clustering of particles. By comparison with numerical simulations, the effect of the correlations is elucidated. Their influence is found to be significant for a free energy that is very concave or has several convex and concave sections. Nevertheless, the ratio of self- and transport diffusion is always close to the thermodynamic factor, $D_t/D_s \approx \Gamma$, a result which is exact in the absence of correlations. Finally, we obtained quantitative agreement between numerical simulations of our model and experimental results of diffusion in ZIF-8 from Ref. [20].

This work was supported by the Flemish Science Foundation (FWO-Vlaanderen).

*thijsbecker@gmail.com

[1] A. Einstein, Ann. Phys. (Berlin) **322**, 549 (1905).
[2] J. B. Perrin, *Atoms* (Constable, London, 1916).
[3] R. J. A. Tough, P. N. Pusey, H. N. W. Lekkerkerker, and C. Van den Broeck, Mol. Phys. **59**, 595 (1986).

[4] J. L. Anderson and C. C. Reed, J. Chem. Phys. **64**, 3240 (1976).
[5] C. Van den Broeck, F. Lostak, and H. N. W. Lekkerkerker, J. Chem. Phys. **74**, 2006 (1981).
[6] C. Van den Broeck, J. Chem. Phys. **82**, 4248 (1985).
[7] R. Zwanzig, J. Phys. Chem. **96**, 3926 (1992).
[8] D. Lucena, D. V. Tkachenko, K. Nelissen, V. R. Misko, W. P. Ferreira, G. A. Farias, and F. M. Peeters, Phys. Rev. E **85**, 031147 (2012).
[9] K. Nelissen, V. R. Misko, and F. M. Peeters, Europhys. Lett. **80**, 56004 (2007).
[10] J. C. N. Carvalho, K. Nelissen, W. P. Ferreira, G. A. Farias, and F. M. Peeters, Phys. Rev. E **85**, 021136 (2012).
[11] R. Gomer, Rep. Prog. Phys. **53**, 917 (1990).
[12] T. Ala-Nissila, R. Ferrando, and S. C. Ying, Adv. Phys. **51**, 949 (2002).
[13] D. A. Reed and G. Erlich, Surf. Sci. **102**, 588 (1981).
[14] P. S. Burada, P. Hänggi, F. Marchesoni, G. Schmid, and P. Talkner, ChemPhysChem **10**, 45 (2009).
[15] M. E. Davis, Nature (London) **417**, 813 (2002).
[16] T. J. Barton, L. M. Bull, W. G. Klemperer, D. A. Loy, B. McEnaney, M. Misono, P. A. Monson, G. Pez, G. W. Scherer, J. C. Vartuli *et al.*, Chem. Mater. **11**, 2633 (1999).
[17] K. S. Park, Z. Ni, A. P. Côté, J. Y. Choi, R. Huang, F. J. Uribe-Romo, H. K. Chae, M. O'Keeffe, and O. M. Yaghi, Proc. Natl. Acad. Sci. U.S.A. **103**, 10186 (2006).
[18] R. Banerjee, A. Phan, B. Wang, C. Knobler, H. Furukawa, M. O'Keeffe, and O. M. Yaghi, Science **319**, 939 (2008).
[19] H. Bux, C. Chmelik, J. M. van Baten, R. Krishna, and J. Caro, Adv. Mater. **22**, 4741 (2010).
[20] C. Chmelik, H. Bux, J. Caro, L. Heinke, F. Hibbe, T. Titze, and J. Kärger, Phys. Rev. Lett. **104**, 085902 (2010).
[21] H. Jobic, J. Kärger, and M. Bée, Phys. Rev. Lett. **82**, 4260 (1999).
[22] L. Heinke, D. Tzoulaki, C. Chmelik, F. Hibbe, J. M. van Baten, H. Lim, J. Li, R. Krishna, and J. Kärger, Phys. Rev. Lett. **102**, 065901 (2009).
[23] F. Salles, H. Jobic, G. Maurin, M. M. Koza, P. L. Llewellyn, T. Devic, C. Serre, and G. Ferey, Phys. Rev. Lett. **100**, 245901 (2008).
[24] N. Rosenbach, H. Jobic, A. Ghoufi, F. Salles, G. Maurin, S. Bourrelly, P. L. Llewellyn, T. Devic, C. Serre, and G. Férey, Angew. Chem., Int. Ed. **47**, 6611 (2008).
[25] D. Tzoulaki, L. Heinke, H. Lim, J. Li, D. Olson, J. Caro, R. Krishna, C. Chmelik, and J. Kärger, Angew. Chem., Int. Ed. **48**, 3525 (2009).
[26] H. Jobic, in *Adsorption and Diffusion*, edited by H. G. Karge and J. Weitkamp (Springer-Verlag, Berlin, Heidelberg, 2008), Vol. 7, pp. 207–233.
[27] R. Krishna and J. M. van Baten, Langmuir **26**, 10854 (2010).
[28] R. Krishna and J. M. van Baten, Langmuir **26**, 8450 (2010).
[29] R. Krishna and J. M. van Baten, Langmuir **26**, 3981 (2010).
[30] See Supplemental Material at http://link.aps.org/supplemental/10.1103/PhysRevLett.111.110601 for more details regarding calculations, simulations, and fit with ethanol.
[31] T. Becker, K. Nelissen, B. Cleuren, B. Partoens, and C. Van den Broeck (to be published).
[32] M. Kardar, *Statistical Physics of Particles* (Cambridge University Press, Cambridge, England, 2007), Chap. 4.
[33] N. G. Van Kampen, *Stochastic Processes in Physics and Chemistry* (North-Holland, Amsterdam, 1981).
[34] C. Chmelik, J. Kärger, M. Wiebcke, J. Caro, J. M. van Baten, and R. Krishna, Microporous Mesoporous Mater. **117**, 22 (2009).
[35] F. Salles, H. Jobic, T. Devic, P. L. Llewellyn, C. Serre, G. Férey, and G. Maurin, ACS Nano **4**, 143 (2010).
[36] R. Krishna and J. M. van Baten, Microporous Mesoporous Mater. **138**, 228 (2011).
[37] R. Krishna and J. M. van Baten, Microporous Mesoporous Mater. **109**, 91 (2008).
[38] J. A. Northby, J. Chem. Phys. **87**, 6166 (1987).
[39] C. Chmelik (private communication).